Journal of Geography, Environment and Earth Science International

Volume 27, Issue 10, Page 113-129, 2023; Article no.JGEESI.107166
ISSN: 2454-7352

Tracing the Sources of Paleoproterozoic Metasediments in the Comoé Basin, Côte d'Ivoire, West Africa : Geochemistry Implication

Koffi Raoul Teha [a*], Koffi Kossonou Jean-Marie Pria [b], Augustin Yao koffi [a], Koffi Joseph Brou [a], Brice Roland Kouassi [c] and Alain Nicaise Kouamelan [a]

[a] Université Félix Houphouët-Boigny Abidjan-Cocody, Laboratoire Ressources Minérale et Energétique (LGRME), UFR STRM, 22 BP 582 Abidjan 22, Côte d'Ivoire.
[b] Département des Sciences de la Terre, Université Jean Lorougnon-GUEDE Daloa, Laboratoire Sciences et technologie de l'environnement, UFR Environnement, BP 150 Daloa, Côte d'Ivoire.
[c] Département de Géosciences, Université Péléforo Gon Coulibaly Korhogo, UFR des Sciences Biologiques, BP 1328 Korhogo, Côte d'Ivoire.

Authors' contributions

This work was carried out in collaboration among all authors. All authors read and approved the final manuscript.

Article Information

DOI: 10.9734/JGEESI/2023/v27i10720

Open Peer Review History:
This journal follows the Advanced Open Peer Review policy. Identity of the Reviewers, Editor(s) and additional Reviewers, peer review comments, different versions of the manuscript, comments of the editors, etc are available here: https://www.sdiarticle5.com/review-history/107166

Original Research Article

Received: 28/07/2023
Accepted: 05/10/2023
Published: 17/10/2023

ABSTRACT

Petrology and geochemistry have been used jointly to study the metasediments of the Comoé Basin. The main objective is to identify the sources of the metasediments. The entire Comoé metasedimentary basin is dominated by greywackes and shales. The mineralogy of the greywackes

**Corresponding author: E-mail: rkteha@hotmail.fr;*

consists of biotite, plagioclase, quartz, muscovite, chlorite, ilmenite and other oxides. The shales contain andalusite, biotite, muscovite, quartz and chlorite. Overall, the geochemistry of the major elements shows an enrichment of Fe_2O_3, MgO, Al_2O_3, K_2O and TiO_2 in the metapelitic rocks. These oxides are controlled by the distribution of phyllosilicates. Observation of diagrams of rare earth elements has shown that the source of these elements in these metasediments for these elements is largely controlled by the TTG. On the other hand, a large quantity of felsic material, in particular felsic rocks, contributed to the composition of the sediments. Mafic rocks contributed to a lesser extent.

Keywords: Côte d'Ivoire; Comoé basin; metasediments; sources; TTG.

1. INTRODUCTION

The West African Craton (WAC) is formed by the Leo-Man shield and the Reguibat shield, separated by the Taoudeni Basin ([1-7], Fig. 1a). It underpins several countries including Côte d'Ivoire. The southern part of the West African Craton is represented by Côte d'Ivoire, which has two basins belonging to the paleoproterozoic domain: the Comoé basin and the Lobo basin ([1], Fig. 1b). The Comoé basin is located to the South-East of the Leo-Man shield. It extends from the south to the north of Côte d'Ivoire and is 17 km thick (Fig. 1b).

Several field and laboratory studies have been conducted [8-11]. These studies have provided insight into the tectonics, classification and origin of the metasediments. The Comoé metasedimentary basin is dominated by metapelites and metaarenites [12]. These rocks are intruded by a variety of granitoids [13-15].

This paper will (i) compare the chemical compositions of the rocks to see if there is any variation in lithology and (ii) trace the sources of the Comoé basin sediments. Arenites and pelites are major groups of metasedimentary rocks. These rocks must be accurately identified by classification. Sampling was carried out on fine-grained rocks. The collected rocks are rich in rare earths and record the intensity of weathering during transport and diagenesis processes. The petrology and chemical composition of major, minor and trace elements are analysed on these metasedimentary rocks in order to assess their chemical composition in space and time. The use of lithogeochemistry will allow us to establish correlations between macroscopically similar, metamorphosed and deformed sedimentary units [16,17]. Mechanically and chemically stable minerals from a source are of great use for this study [18].

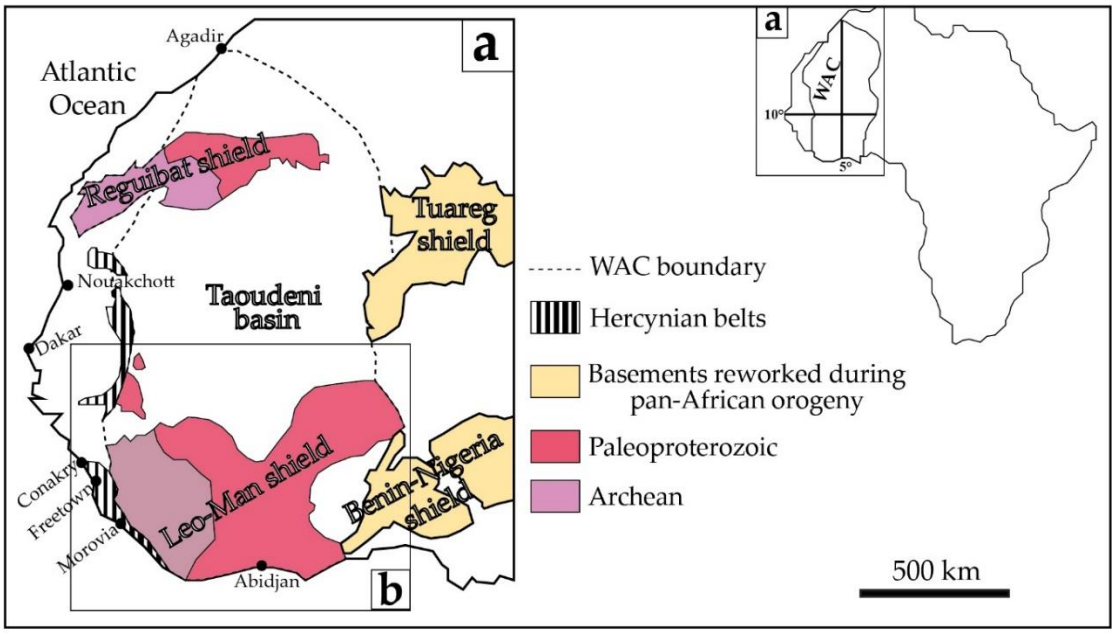

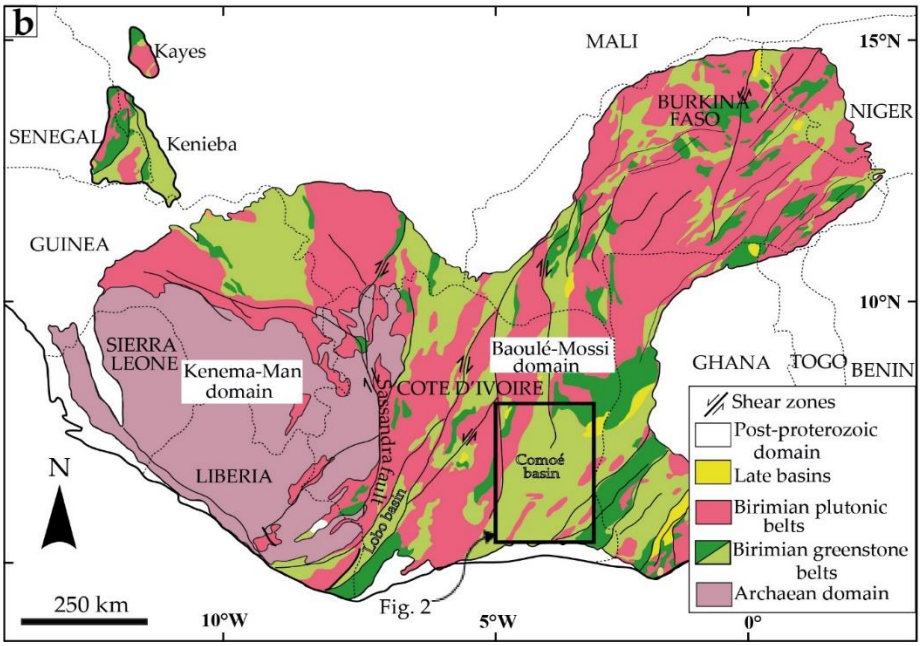

Fig. 1. Regional geologycal maps

a) Geological sketch map of the West African Craton (WAC) (modified after [19, 20]). The map shows the capitals of the countries. b) Simplified geological map of Leo-Man shield (modified after [21, 22]), location of Comoé basin in the South-East part of Leo-Man shield

1.1 Geological Setting

The Leo-Man ridge consists of the Kenema-Man domain and the Baoulé-Mossi domain [23-25]. The two domains are separated by the Sassandra shear zone [26]. The Kenema-Man domain is located west of the Sassandra shear zone. It composed of tonalite-trondhjemite-granodiorite (TTG) plutons, extensive gneissic domains and volcano-sedimentary meta belts [27,4,28,29]. The metavolcanic-sedimentary belts are delimited by shear zones and alternate with TTG granitoids and gneissic domains.

The Baoulé-Mossi domain is also called the Paleoproterozoic domain. It is located to the east of the Sassandra shear zone and covers a large part of the Leo-Man shield. This vast domain is made up of deformed and metamorphosed volcanic, volcano-sedimentary and metasedimentary rocks. These rocks are intruded by several generations of granitoids with alkaline, calc-alkaline geochemical signatures and peraliminous [30-33,13].

1.2 Geology of Comoe Basin

The study area consists of volcano-sedimentary, meta-sedimentary and granitoids intrusions (Fig. 2). The Comoé domain is located to the South-East of the Palaeoproterozoic domain. The lithostratigraphy of the Comoé unit is essentially composed of quartzites, basic to acid vulcanites [34], shales and sandstones [35,36] resting unconformably on an antebirimian granito-migmatitic basement. Volcanic formations are very little represented and essentially on the periphery.

The metasediments are composed of sericitoschistes, chloritoschistes and poundingues, with compositions of quartz arenite, litharenites and sandstone (arkose and ferruginous sandstone) [10]. The petrographic and structural study permits to characterize, in part, thirteen different facies of granitoids in the Tiassalé region (southern Côte d'Ivoire) [14]. The absence in the region of gneiss and migmatites, the presence of enclaves of varied petrographic type in the studied different facies, in favor of the hypothesis of a mantle or mixed origin of the the magmas for these granitoid facies [14]. For [13], the absence of contact metamorphism indicates that the sedimentary series must be deposited on these granites. These massifs may correspond to the complex TTG units of the Nassian domain that were emplaced very early during eburnean history. The protoliths of metasediment are ranging from gabbro to granodiorite, all have been affected by strong to moderate alteration ($62 < CIA < 97$) [9,10].

2. ANALYTICAL METHODS

Petrography and geochemical analysis are the main methods used to achieve these objectives.

2.1 Petrography

The petrographic study of the rocks was carried out by traversing the region from north to south. Petrography consisted in describing the lithological units observed in the various outcrops encountered. Eight thin sections were prepared at the Laboratoire des Sciences de la Terre et des Ressources Minières (UFR-STRM) of the Université Félix Houphouët Boigny d'Abidjan - Cocody. The samples are located on the litho-structural map. They are numbered MS01 to MS08 (Fig. 2).

2.2 Geochemistry

The chemical composition was determined in the BUREAU VERITAS laboratory. Eight metasedimentary rocks from the Comoé basin were analysed (Table 1). ICP-AES and ICP-MS methods were used to determine major and trace elements respectively. Sample preparation consists of grinding some of the fresh rock into powder. To do this, the samples are sawn, washed several times to remove the dust and dried in an oven. The loss on ignition is measured. It allows the degree of weathering, water and carbonate content to be quantified. The loss on ignition is determined according to the formula :

$$\text{Loss on ignition} = \frac{\text{Sample weight} - \text{Calcined sample weight}}{\text{Sample weight}} \times 100$$

The geochemical data was used to draw up diagrams that provide information on the geochemical characteristics and geotectonic environments of the petrographic facies.

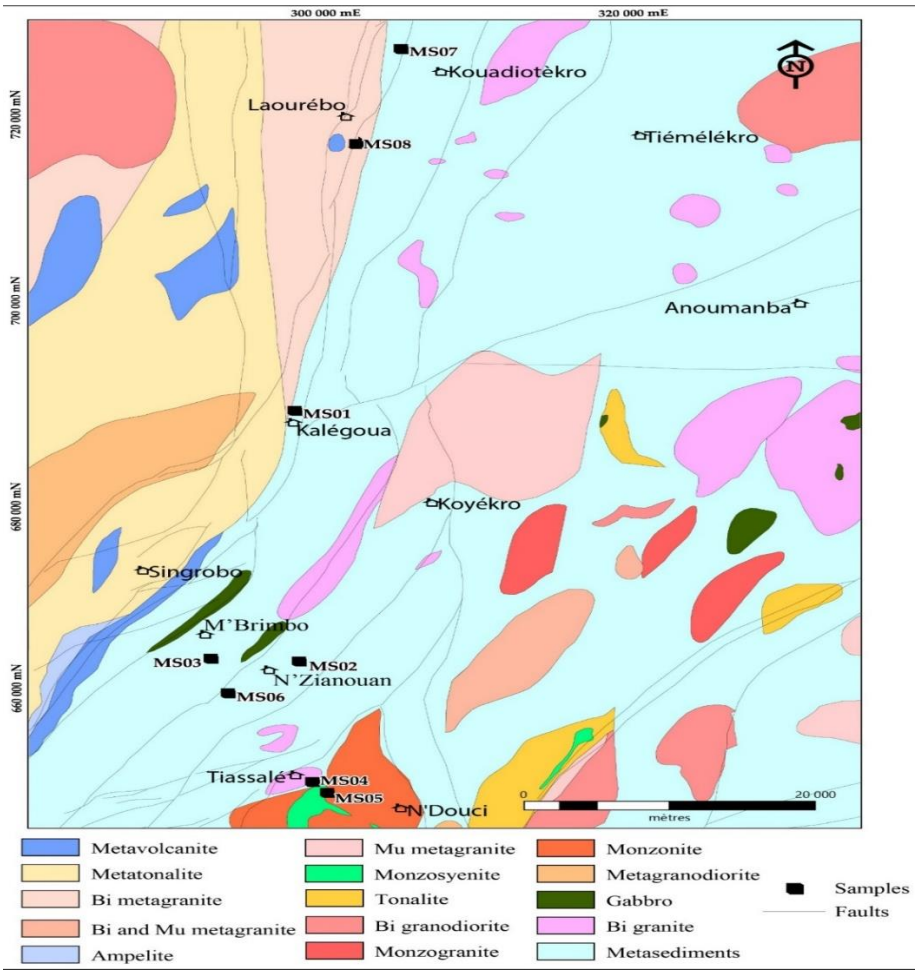

Fig. 2. Litho-structural map of the Comoé basin [12], modified
Black squares show the location of the studied rocks of the Comoé basin

Table 1. Whole rock major and trace element composition

Samples	MS01	MS02	MS03	MS04	MS05	MS06	MS07	MS08	DL[a]
WGS84 Coordonate system									
Lat	4.8276	4.82413	4.87888	4.81556	4.80633	4.86814	4.76283	4.79122	
Long	-6.23777	-6.00401	-6.0064	-5.89161	-5.88159	-5.97422	-6.57521	-6.48758	
Wt%									
SiO_2	68.8	68.9	71	63.4	57.82	53.82	68.4	63.4	0.01
TiO_2	0.61	0.47	0.53	0.78	0.91	0.78	0.56	0.7	0.001
Al_2O_3	13.4	13	12.7	17.9	20.71	21.91	14.7	17.5	0.01
Fe_2O_3	6.54	4.59	5.1	7.48	7.29	9.06	5.25	7.04	0.01
MnO	0.1	0.06	0.06	0.07	0.05	0.07	0.07	0.08	0.001
MgO	2.27	1.38	1.44	2.75	2.54	3.39	2.01	2.69	0.01
CaO	2.22	2.9	1.57	1.73	0.59	1.11	1.38	1.31	0.01
Na_2O	3.19	3.25	3.37	3.48	1.53	2.01	3.35	2.3	0.01
K_2O	1.18	1.49	1.57	2.13	3.67	4.08	1.83	2.9	0.01
P_2O_5	0.12	0.11	0.12	0.16	0.09	0.14	0.12	0.22	0.01
LOI	1.25	3.21	1.96	0.74	3.68	4.15	2.64	2.23	0.01
Total	99.68	99.36	99.42	100.62	98.9	100.52	100.31	100.37	
Ppm									
Cs	3.1	2.7	2.6	4	6.4	8.5	3.3	3.5	0.1
Rb	49.9	57.2	58.5	82.7	146.5	155.6	76.4	93.4	1
Ba	451	422	359	653	978	856	474	726	2
Th	3.8	3.5	3.8	4	4.3	5.0	5.2	4.3	0.05
Nb	5	4	4.4	6.1	8.1	6.7	5.4	6.8	0.2
Pb	1.5	5.9	2.7	1.5	8.9	2.6	5.2	2.1	0.1
Sr	266.9	355.9	258.1	574.2	237.1	188.1	353.8	241.6	2
Zr	156.7	120	135.3	130.6	162.7	143.4	156.6	145	1
Y	14.9	10.9	17.6	15.3	21.6	18.8	11.1	15.6	0.5
Co	21.1	10.6	13.4	25.2	9.5	27.9	17	22.3	0.1
Ni	50.4	30.6	38.8	65.7	15.8	83.9	38.7	53.5	0.1
Cu	38	18.6	27.3	22.1	22.0	42.7	23.6	30.7	1
Zn	57	42	41	67	96	95	57	84	5
Ga	13.9	11.2	10.6	19.8	25.2	23.8	16.4	20.6	5
Hf	4.2	3.2	3.6	3.4	4.2	3.9	4.1	3.5	0.1

Samples	MS01	MS02	MS03	MS04	MS05	MS06	MS07	MS08	DL[a]
Sn	<1	<1	<1	<1	1	<1	<1	<1	1
Ta	0.4	0.4	0.4	0.5	0.6	0.5	0.5	0.4	0.01
U	1	0.9	0.7	1.4	1.3	1.8	1.2	1.3	0.01
La	21.7	18.2	25.6	20.4	43.4	25	25.1	24.6	0.05
Ce	40.6	37.1	40.4	41.8	81.2	52.9	46.8	52.6	0.05
Pr	5.43	4.45	5.59	5.07	9.83	6.43	5.3	5.75	0.01
Nd	20.3	17.4	20.6	19.9	35.2	25.5	19.7	22.4	0.05
Sm	3.73	3.19	3.65	3.84	6.2	4.84	3.51	3.92	0.01
Eu	1	0.88	1.03	1.08	1.6	1.19	0.95	1.1	0.005
Gd	3.21	2.57	3.53	3.3	5.25	4.06	2.88	3.42	0.01
Tb	0.46	0.38	0.5	0.5	0.79	0.59	0.42	0.52	0.01
Dy	2.53	2.04	2.82	2.71	4.24	3.48	2.3	2.75	0.05
Ho	0.56	0.42	0.61	0.53	0.85	0.71	0.46	0.64	0.01
Er	1.57	1.23	1.59	1.57	2.41	2.03	1.26	1.78	0.01
Tm	0.24	0.2	0.23	0.22	0.38	0.32	0.19	0.26	0.05
Yb	1.59	1.17	1.44	1.53	2.41	2.02	1.37	1.8	0.01
Lu	0.24	0.18	0.23	0.23	0.38	0.32	0.21	0.27	0.002
Ti	0.2	<0.1	<0.1	0.4	0.1	0.1	<0.1	0.2	0.1
Eu/Eu*	0.89	0.94	0.86	0.83	0.92	0.93	0.89	0.94	
Ce/Ce*	0.88	0.97	0.92	0.98	0.95	1.04	0.79	0.97	
La/Yb	9.01	10.27	11.89	8.17	12.10	9.02	11.74	8.80	
La/Sm	3.55	3.48	4.27	3.15	4.36	3.83	4.28	3.24	
Gd/Yb	1.62	1.76	1.75	1.61	1.69	1.53	1.97	1.73	
CIA[b]	67.03	62.98	66.11	70.92	78.15	75.27	69.14	72.89	

a : Detection Limit
b : Chemical Index of Alteration

3. RESULTS AND DISCUSSION

3.1 Results

The main results of the petrographic and geochemical data are highlighted in this section.

3.1.1 Petrography characteristic

Metasedimentary rocks are observed in the Bandama (Fig. 3a) and N'Zi (Fig. 3b) rivers. These are rocks that form alignments of sometimes thin bands. The outcrops have a foliated appearance, generally derived from arenites with relatively abundant cement (20%). The main foliation S1 is N-S to NNE-SSW trending with subvertical dips (Fig. 3). In this section, we have distinguished between the metasediments of the Tiassalé group and those of the Toumodi group.

3.1.1.1 Metasediments of the Tiassalé group

The Tiassalé sector includes the localities of Tiassalé, M'Brimbo and N'Zianoua. We collected five metasedimentary rocks in this area (MS02, MS03, MS04, MS05 and MS06). Macroscopically, these samples are dark-green, fine-grained and foliated. They are composed of greywacke (MS02 and MS03) and orthoschist (MS04, MS05 and MS06). The greywacke consists of 40% quartz, 35% plagioclase and 20% biotite. Quartz and plagioclase crystals are subrounded. Accessory minerals are mainly represented by oxides (Fig. 4a). The shales show a variety of compositions (Fig. 4b and c). Sample MS04 is an andalusite micaschist. It consists of small micas crystals (biotite and muscovite) reaching 50% and quartz (40%). The coarse grains are andalusite (5%). Micas form the main minerals of the S1 main foliation (Fig. 4b). The foliation in the orthoschist is materialised by brown biotite and muscovite, which represent 60% of the minerals in the rock. The mica beds alternate with quartz (35%) (Fig. 4c).

3.1.1.2 Metasediments of the Toumodi group

This group includes the localities of Kalégoua, Laourébo and Kouadiotèkro. We collected three samples in the Toumodi area (MS01, MS07 and MS08). The metasediments are dense, very coherent, with a fine texture (Fig. 4d, e and f). Samples MS01 and MS07 are greywackes with contrasting mineralogical compositions (Fig. 4d and e). Chlorite and muscovite represent 70% of the minerals in sample MS01 (Fig. 4d). Together with the quartz (25%) beds they form the foliation in the rock (Fig. 4d). Accessory minerals are ilmenite (5%) (Fig. 4d). However MS07 is very abundant in quartz of various sizes (60%) (Fig. 4e). The quartz crystals are surrounded by fine beds of brown biotite (30%) (Fig. 4e). Accessory minerals are oxyde (3%) (Fig. 4e). Sample MS08 is composed of chlorite (35%), quartz (30%), muscovite (20%) and biotite (15%). These minerals are the main foliation of the rock (Fig. 4f). The coarse grains are staurotite, moulded by the S1 foliation (Fig. 4f).

3.1.2 Geochimical characteristic

3.1.2.1 Classification of Comoé metasediments

In this section, we used several diagrams to discriminate the metasedimentary rocks of the Comoé. According to the classification diagram $Log(Fe_2O_3/K_2O)$ versus $Log(SiO_2/Al_2O_3)$, proposed by [37], the samples of the Tiassalé and Toumodi groups are related to greywackes and shales (Fig. 5a).

In Fig. 5b, these metasedimentary rocks show mostly alkaline affinities in the $(Na_2O+CaO)/K_2O$ versus SiO_2 diagram [38]. However, some samples (shale) from the Tiassalé group show potassic characteristics (Fig. 5b). The variation of K_2O/Na_2O versus SiO_2 ratios (Fig. 5c), in the discrimination diagram of [16], places the samples of the Toumodi group and some of the Tiassalé samples in the active continental margin field. Some samples (shales), mainly those from Tiassalé, are in the island arc field.

3.1.2.2 Major oxides

The degree of alteration of the metasediments during chemical weathering is determined from the Chemical Index of Alteration (CIA) diagram [39]. CIA is calculated from the molecular proportions:

$CIA = [Al_2O_3/(Al_2O_3 + CaO^* + Na_2O + K_2O)] x100.$

CaO^* is the concentration of CaO incorporated in the silicate fraction of the rock. The diagram in Fig. 6a shows the results of the calculation of the Chemical Index of Alteration.

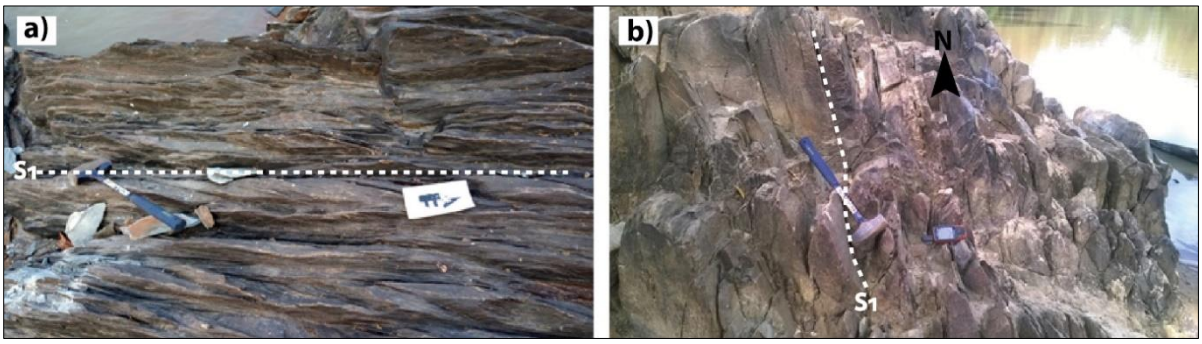

Fig. 3. Foliated metasedimentary rocks in the Bandama and N'Zi river beds
a) NNE-SSW oriented millimetre thin bands make up the Bandama metasediments. b) NNE-SSW foliation observed in the decimetric beds of the N'Zi River

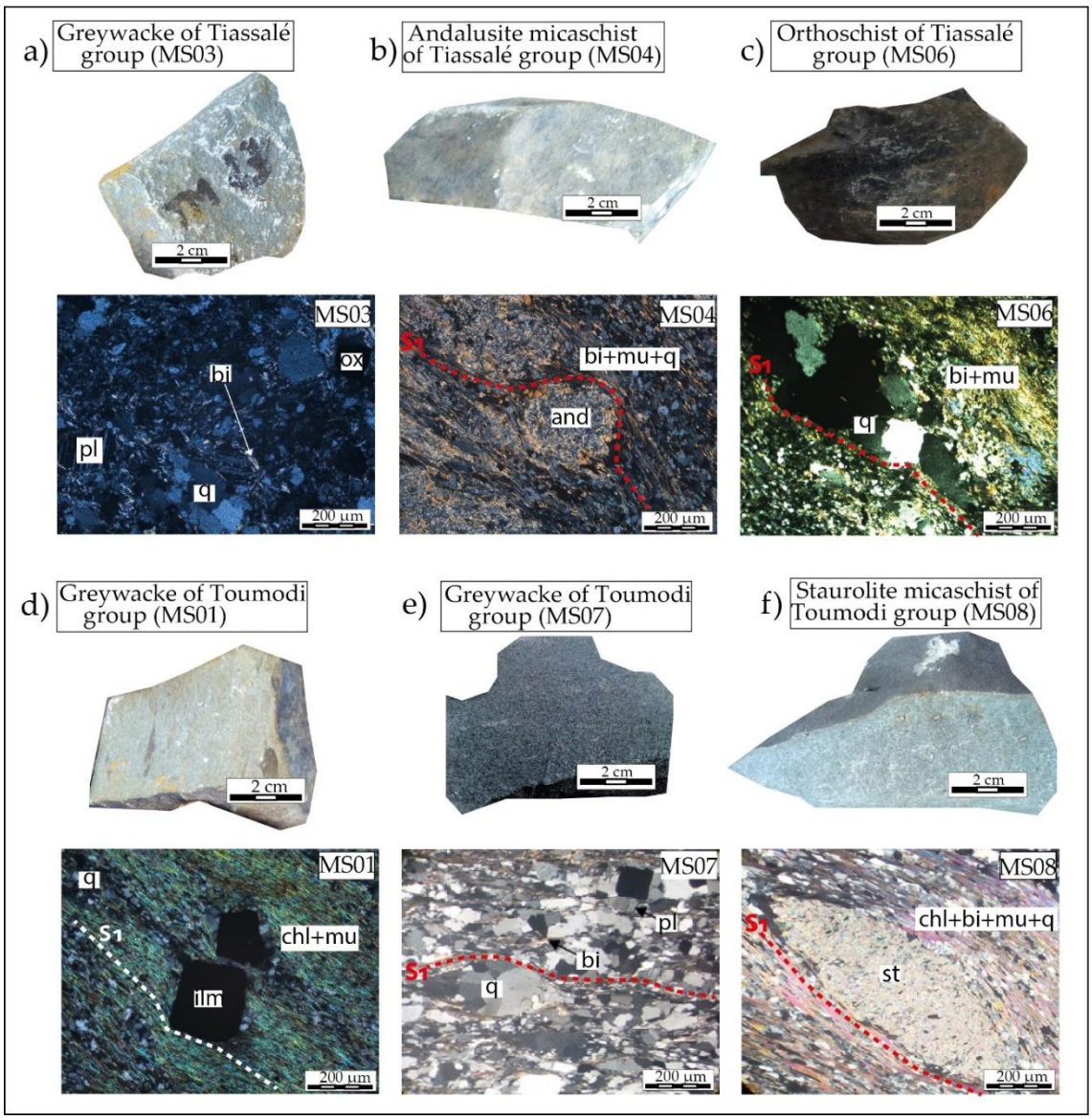

Fig. 4. Photographs and microphotographs of studied metasedimentary rocks of Comoé basin.
Abbreviations : MS01 = Sample identification ; q = quartz ; pl = plagioclase ; bi = biotite ; and = andalusite ; mu = muscovite ; ox = oxide ; ilm = ilmenite ; chl = chlorite ; st = staurolite

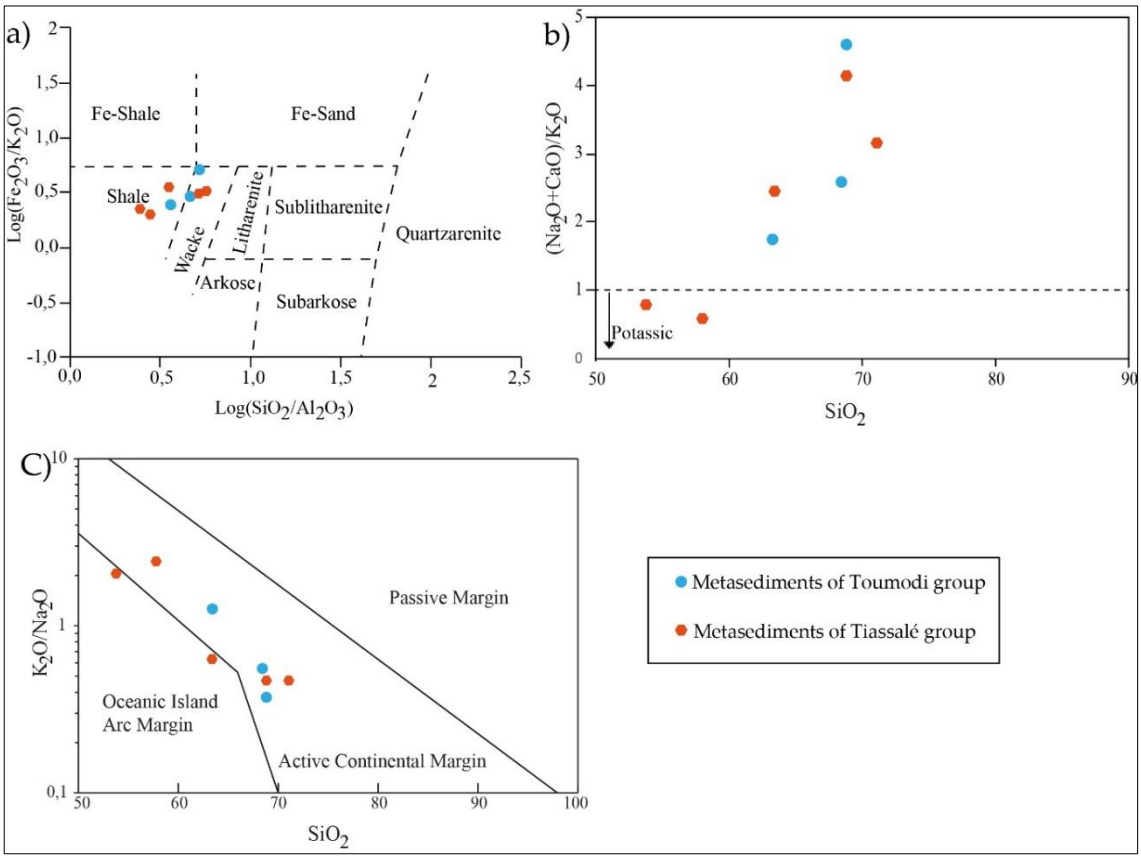

Fig. 5. Discrimination diagrams of the metasedimentary rocks of the Comoé basin.

a) Log(Fe_2O_3/K_2O) versus Log(SiO_2/Al_2O_3) diagram according to [37]. The metasediments are composed of greywackes and shales; b) Diagram (Na_2O+CaO)/K_2O versus SiO_2 showing the alkaline and potassic characters of the metasediments, after [38] ; c) Discrimination diagram of K_2O/Na_2O versus SiO_2 of the geotectonic context of the metasediments, after [16]

The general trend indicates an increase in the chemical index of alteration in the Comoé metasediments. This index is above 78. For metasediments with SiO_2 contents between 65-75%, the chemical index of alteration varies from 60 to 70. SiO_2 contents of 53-63% show chemical index of alteration of 70-80. The chemical index of alteration between 60-80 reflects low to moderate alteration of the source rock [40,41]. In addition, the compositional poles of the source rocks (TTG and mafic rocks) have lower index than the metasediments. However there is a negative correlation between the chemical index of alteration of metasediments, felsic rocks and SiO_2. The approximately linear distribution indicates the intervention of a felsic source. The shales of the Tiassalé Group have the highest indexes. The material of these rocks is more altered than the other rocks of the basin.

In detail, the samples vary inversely with silica content (Fig. 6b, c). There is an increase in Fe and Mg in the metasediments. Some samples of Tiassalé shale are rich in Fe (about 10%, for a SiO_2 content of 53.82%). They are similar to mafic rocks. The SiO_2 vs MgO diagram indicates that the Fe-rich samples are also enriched in Mg. In both diagrams, there is an excellent correlation between the metasediments and the TTG. However, in the SiO_2 vs. Fe_2O_3 diagram, this negative correlation is also associated with mafic and felsic rocks. The linear trend of the rocks would indicate that the metasediments come from the same source.

In the diagram in Fig. 6d, the correlation is negative between metasediments, TTG and felsic rocks. Al_2O_3 content varies inversely with silica. There is a high proportion of aluminium-rich minerals. Aluminium content varies between 10% and 25%. Samples rich in Al_2O_3 are the poorest in SiO_2. These aluminium-enriched samples suggest the presence of aluminous minerals such as kaolinite in the initial sediments [42,43].

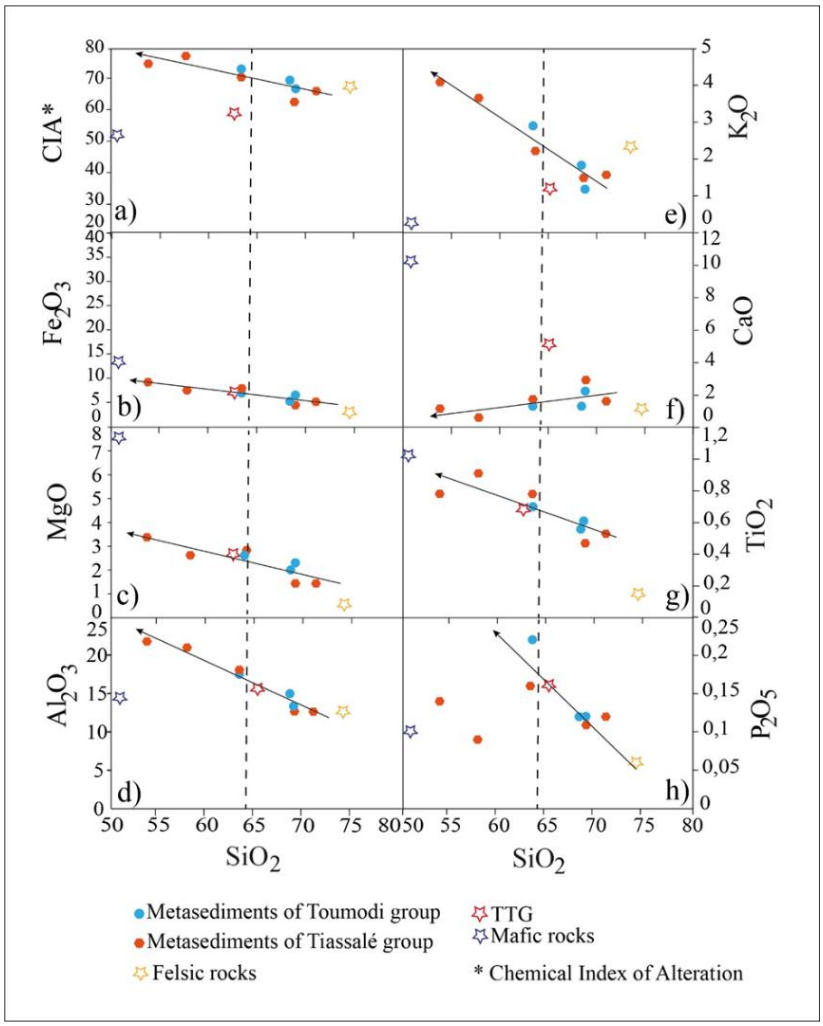

Fig. 6. Distribution of metasediments in SiO_2 vs oxide diagrams of Harker

The black arrow indicates the enrichment or depletion of oxides relative to silica. The stars represent the location of mafic, felsic and TTG rocks. The dotted vertical line corresponds to the boundary between shales and greywackes

The SiO_2 vs K_2O diagram also shows a negative correlation (Fig. 6e). K_2O is a component of white micas and alkali feldspars. The slope indicates a gain in potassium in the residual alteration minerals [42]. Similarly, SiO_2 vs TiO_2 and SiO_2 vs P_2O_5 show negative slopes. However, a slight dispersion can be seen in the diagram in Fig. 6h. TiO_2 and P_2O_5 are considered to be immobile elements during weathering. TiO_2 would be contained in the ilmenite described in the petrography. The slight enrichment in P_2O_5 suggests that apatite and monazite are present in greater quantities. Both diagrams show a relationship between metasediments and TTG. There is also a good correlation between metasediments, mafic rocks (Fig. 6g) and felsic rocks (Fig. 6h). The TTG could be the source of the metasediments, with mafic and felsic material participating. This observation will be verified with the following diagram.

The diagram in Fig. 6f shows a positive correlation between SiO_2 and CaO. However, there is no correlation between the metasediments and the felsic, mafic and TTG rocks. In this diagram, the positive slope indicates a loss of CaO in the alteration solution.

3.1.2.3 Rare earth elements

The chemistry of the metasediments shows La contents ranging from 18.2 to 43.4 ppm, Ce from 37.1 to 81.2 ppm, Pr from 4.45 to 9.83 ppm and Nd from 17.4 to 35.2 ppm (Tab. 1). The HREE show lower values than the LREE. The rare-earth spectra of metasediments normalized to

the chondrites of [44], indicate a moderate fractionation in LREE, reflected by their ratio (La/Sm)n between 3.15 and 4.36. The (Gd/Yb)n ratio is in the range 1.53-1.97, suggesting sub-flat HREE spectra. The metasediments show enrichments in light rare earths relative to the chondrite of the order of more than 55 to more than 100 times for La, 45 to 100 times for Ce, 35 to 90 times for Pr and 30 to 65 times for Nd. The contents of heavy rare earths (Er, Tm, Yb) are grouped together and do not exceed 15 times the in the chondrite. There is also a small negative anomaly in Eu (Eu/Eu* = 0.83-0.95) (Fig. 7). The almost identical spectra suggest that the metasediments may have the same sources, with slight variations.

3.1.2.4 Characterisation of the source of metasediment

Some rare earth elements and other elements with a high ionic potential are characterised by their low mobility, small size and high electronic charge. Zircon contains a portion of these elements transported in sedimentary rocks during alteration and transport. They reflect the signature of the parent material [45,42]. These elements will be used to determine the source of the metasediments and the provenance of the clastic sediments.

The diagrams in Fig. 8 use constituents from mafic rocks (TiO_2, Y) and felsic rocks (Zr). In Fig. 8a (Zr vs. TiO_2), the metasediment samples are outside the field defined by the TTGs, mafic and felsic rocks. They cluster around the TTG. A wide dispersion is observed in the Y vs. TiO_2 diagram (Fig. 8b). The samples are closer to the poles of the TTG and mafic rocks. In both diagrams, zirconium (Zr), yttrium (Y) and titanium (Ti) are elements controlled by sources close to the TTG that have been diluted by a mafic source.

Trace elements are also influenced by their source, erosion and diagenesis [38]. Like Zr, Hf is an immobile element that is distributed mechanically. Their concentration depends on the heavy minerals. Th is transported in clasts and reflects the geochemistry of the source [38]. The Th vs U binary digram shows a good distribution and correlation (Fig. 9a). U/Th ratios range from 0.18 to 0.36. The chondritic ratio is around 0.28.

The Hf vs Zr diagram in Fig. 9b also shows a good distribution and a positive correlation. Zr/Hf ratios are generally greater than 36 (chondritic ratio). The trace elements used in these two diagrams reflect signatures characteristic of a felsic source (TTG).

There are two trends in the La vs Th diagram (Fig. 9c). The first trend shows a high La/Th ratio of 10.09. This ratio reflects Th depletion in some metasediments. The second trend shows a slight enrichment in Th. The La/Th ratio is 6.53. This diagram shows that a large quantity of felsic material contributed to the formation of the sediments in the Comoé basin. Both trends would explain the distinct tectonic environments [46].

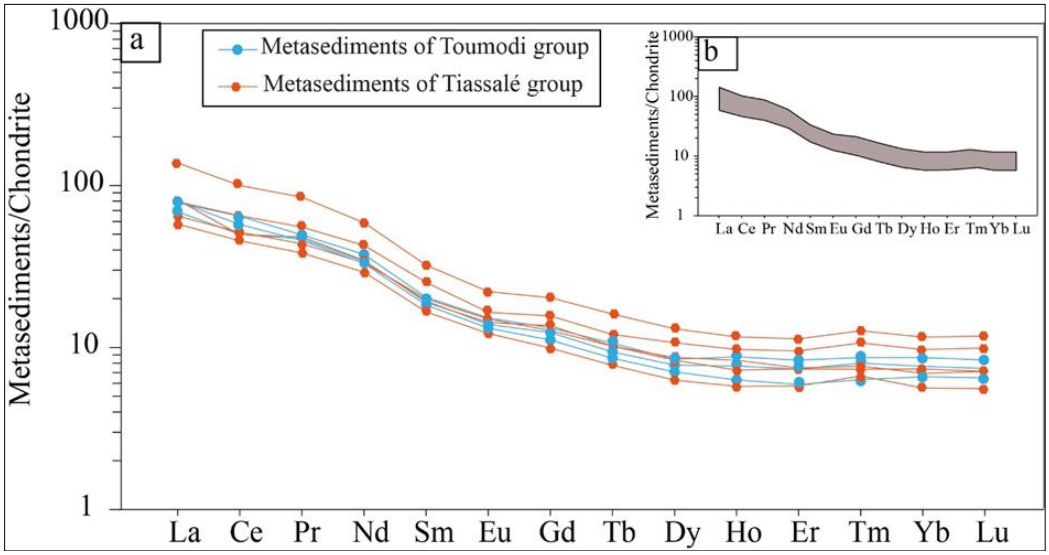

Fig. 7. Rare earth spectra

a) Rare earth spectra of metasediments normalized to chondrites, [44]. b) General trend in metasediment spectra

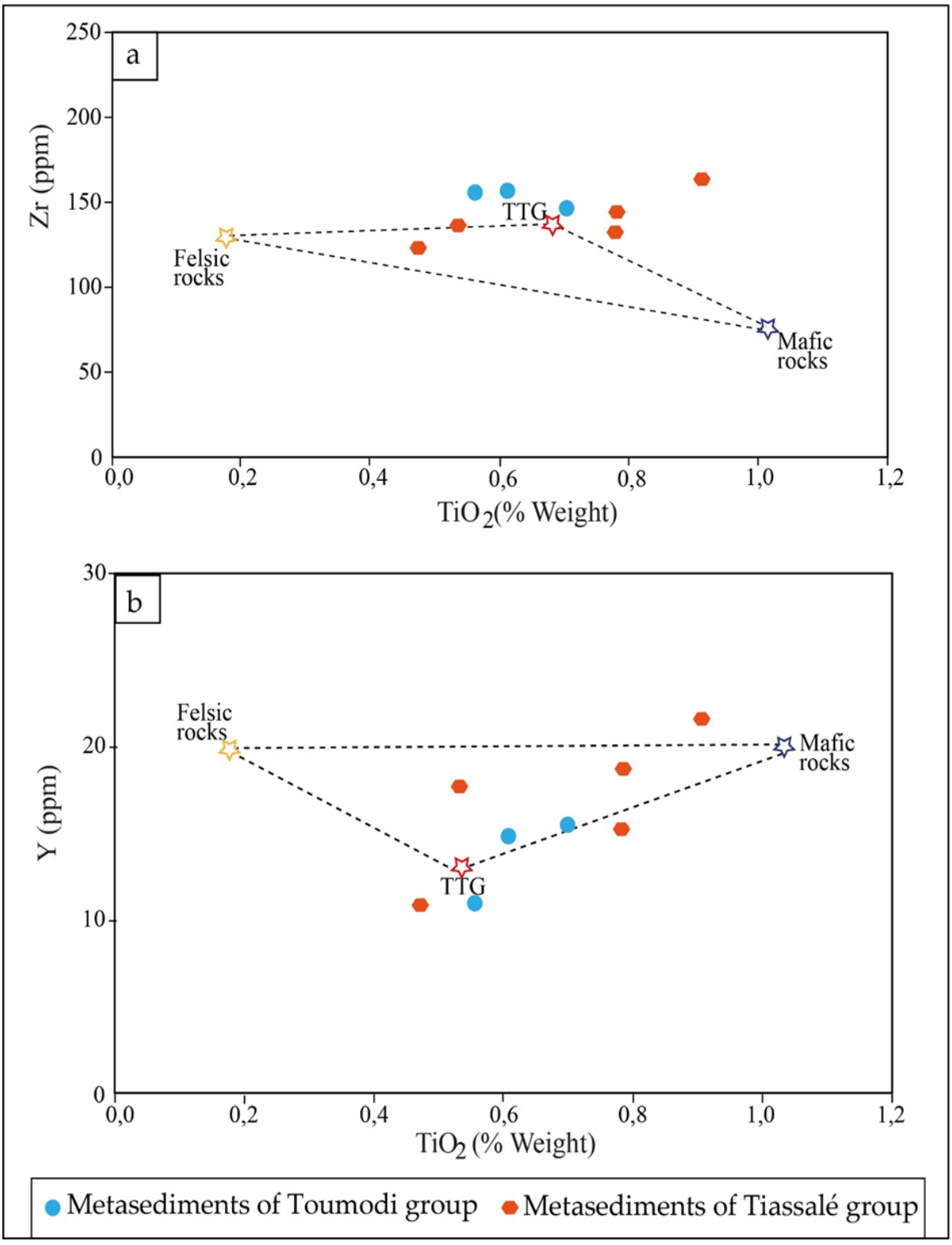

Fig. 8. Source identification diagrams, after [38], modified

a) Zr vs TiO_2 ; b) Y vs TiO_2. The stars represent the location of possible sources

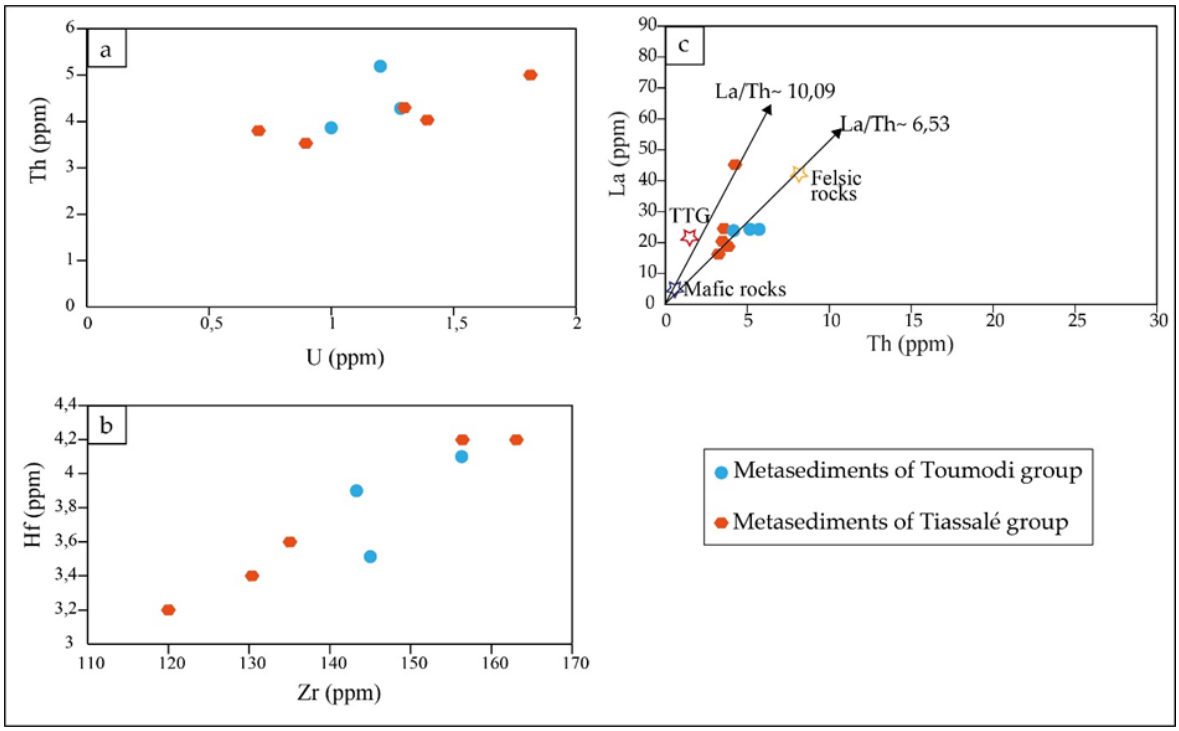

Fig. 9. Trace element variation diagrams for metasedimentary rocks

a) Th vs U ; b) Hf vs Zr ; c) La vs Th to determine the source of the initial sediments, the black arrows represent the increase in La and the increase in Th

3.2 Discussion

Petrographic studies of metasediments have revealed greywack, shale and micaschist in the Comoé Basin. These metasedimentary rocks are also highlighted by [9], in the SASCA transition zone by [47], and in southern Ghana by [48].

The geochemical aspect indicates low to moderate CIA, similar to the metasediments described in north-eastern Canada [49]. The enrichment of Fe_2O_3, MgO, Al_2O_3, K_2O and TiO_2 indicates that the Comoé basin has a mafic component in its composition and a volume of clay minerals. The P_2O_5 enrichment suggests a large quantity of minerals resistant to alteration, such as apatite and monazite [42] This volume of minerals can be explained by a proximal source or a source rich in P_2O_5. CaO depletion reflects a small proportion of calcium plagioclase. However, there is an increase in NaO_2. This enrichment reflects a greater input of felsic material or a proximal source.

Diagrams using rare earths and trace elements are the most discriminating. Slight variations can be observed in the rare earth profiles. The factor that justifies these variations in rare earth profiles in metasedimentary rocks is their origin [50,51]. Rare earth profiles revealed slight negative anomalies in Eu, like the metasediments described by [42,38]. This trend towards negative Eu anomalies in metasediments suggests that the source was derived from a fractionated magma [52]. The weak Eu anomaly also reflects the erosion of a high relief followed by a relatively short transport [38]. Plagioclase minerals are therefore preserved in certain metasediments. Interpretation of the diagrams suggests that the composition of the metasediments in the Comoé basin is mainly controlled by the TTG at source. However, a non-negligible quantity of mafic and felsic material have contributed to the composition of the metasediments. These observations were made in the Kumasi basin by [48, 53]. Indeed, after modelling the source of the Kumasi Basin shales, [53] showed that it is composed of 62% TTG, 22% basalt and a minority of granite. Conversely, [9] and [10] have respectively shown that the protoliths of metasediments are closer to gabbros and evolve towards granites and granodiorites. Based on the work of [54], a fractionated LREE model with an almost flat HREE trend and low to moderate Eu anomalies (Eu/Eu* = 0.83 to 0.95) could indicate that feldspar granite-granodiorite is a likely composition in the provenance.

Finally, the geochemical data show that the majority of the metasediments were formed on active continental margins and a minority on the margins of oceanic island arcs. This dual tectonic environment has contributed to the formation of metasediments in Côte d'Ivoire [55-57,9,47,10], in India [58] and Canada [42]. These tectonic environments could suggest that the sediments accumulated at different times. This observation needs to be corroborated by U-TH-PB isotopic studies [59]. The aim of this work is to model the source of the Comoé metasediments more accurately.

4. CONCLUSION

A petrographic and geochemical study of the Comoé basin was carried out to determine the composition and origin of the sediments. This study provided evidence of the existence of varied lithologies within the same basin. Petrography revealed shales and greywackes with varied mineralogical compositions. The metasediments have alkaline and potassic affinities. A chemical alteration index of between 60 and 80 indicates atmospheric alteration of the source rocks. The composition of metasediments in the Comoé basin is controlled mainly by the presence of TTG at source. A rich quantity of mafic and felsic material also contributed to the formation of the metasediments. The Comoé metasediments were emplaced in the context of an active continental margin and an oceanic island arc margin.

ACKNOWLEDGEMENTS

This work is the result of thesis work by T.K.R. and P.K.K.J.-M. It received financial support from the T2GEM project (Geophysical and Geochemical Technologies for Mining Exploration). We would like to thank Kouamé Junior for his involvement in the production of this paper.

COMPETING INTERESTS

Authors have declared that no competing interests exist.

REFERENCES

1. Tagini B. Structural sketch of Ivory Coast. Regional geotectonics test. Doctoral thesis Fac. Sci. Univ. Lausanne. Rapp. SODEMI. Abidjan. 1971; 266.
2. Papon A. Geology and mineralization of South-West Ivory Coast. Summary of the work of the SASCA operation (1962-1968), Abidjan. SODEMI. 1973. and Mem. B.R.G.M. No. 80. 1973; and Bull. Dir. Mines and Geol. 1973. 285.
3. Yacé I. Eburnean volcanism in the central and southern parts of the Precambrian Fettekro chain in Ivory Coast. State thesis, ès Sci. University of Abidjan, 1976 ;376.
4. Camil J. Petrography, chronology of Archaean granulitic groups and associated formations in the Man region (Ivory Coast). Implications for the geological history of the West African craton. Doctor of Science thesis. Univ. Abidjan. 1984;306.
5. Vidal M. Eburnean deformations of the Birimian unit of Comoé (Ivory Coast). J. Afr. Earth Sci. 1987;6(2) :441-152.
6. Pothin KBK. Georgraphy and geochemistry of the Precambrian formations of the Odienne region (North-West of the Ivory Coast). Doctor of Science thesis. Univ. Abidjan. 1988;349.
7. Fabre R, Morel B. Stratigraphy of Birimian units in central Ivory Coast (West Africa). Bull. Soc. Geol. France. 1993;164 (4):609-921.
8. Vidal M, Delor C, Pouclet A, Siméon Y, Alric G. Geodynamic evolution of West Africa between 2.2 Ga and 2 Ga; the “Archaean” style of the green belts and Birimian sedimentary complexes of the northeast of Ivory Coast. Bulletin of the French Geological Society. 1996;167 :307–319.
9. Adingra MPK, Coulibaly Y, Ouattara Z, Coulibaly I. Petrographic and geochemical characteristics of the metasediments of the southeastern part of the Comoé basin (north of Alépé-southeast of the Ivory Coast). REV. RAMRES - 2018;6(2). ** ISSN 2424-7235.
10. Boya TKLD, Kouadio FJLH, Adingra MPK, N'Gatta KGL, Kouamelan AN. The metasediments of Kouassi Bilékro, S/P of Kouassi Datèkro, Eastern Ivory Coast: An example of petrogenesis complex within the Comoé basin. Africa Science. 2022;20(6):57 – 71. ISSN 1813-548X.
11. Koffi KD, Kouassi BR, Allialy ME, Houssou NN, Pria KKJM. Paleoproterozoic evolution of the northeast of the Ivory Coast (West African craton): petro-geochemical study of the metasediments of the Bondoukou-region Tanda. Rev. Ivory. Sci. Technol. 2022;39:167-182 167 ISSN 1813-3290.
12. Delor C, Daouda YB, Simeon Y. Diaby I, Gadou G, Kohou P, Konan G, Dommaget

A, Tastet J. P. Geological map of the Ivory Coast at 1/200,000, Abidjan sheet Ministry of Mines and Energy, Directorate of Geology, Abidjan, Ivory Coast, first edition. 1992;6.
13. Vidal M, Gumiaux C, Cagnard F, Pouclet A, Ouattara G, Pichon M. Evolution of a Paleoproterozoic “weak type” orogeny in the West African Craton (Ivory Coast)", Tectonophysics. 2009;477 :145–159.
14. Ouattara G, Koffi GB. Typology of granitoids from the Tiassalé region (Southern Ivory Coast - West Africa): Structurology and Genetic Relations, Afr. Sc. 2014;10 (2) :258–276.
15. Teha KR, Kouamelan AN, Allialy ME, Djro SC, Houssou NN, Koffi YA, Pria KK, JM, Kouassi B. R, Koffi GRS. Petrographic and geochemical characters of the Birimian granitoids of the Comoé basin and surroundings (South of the Coast d'Ivoire) " International Journal of Engineering Science Invention (IJESI). 2018;7(12) :16-25.
16. Roser BP, Korsch RJ. Provenance Signatures of Sandstone-Mudstone suites determined using discriminant function analysis of major-element data. Chemical Geology. 1988;67:119–139.
17. Fralick PW, Kronberg BI. Geochemical discrimination of clastic sedimentary rock sources. Sedimentary Geology. 1997;113 :111 - 124.
18. Yang S, Wang Z, Guo Y, Li C, Cai J. Heavy mineral compositions of the Changjiang (Yangtze River) sediments and their provenance-tracing implication. Journal of Asian Earth Sciences; 2009;35 :56-65.
19. Grenholm M. The Birimian event in the Baoulé Mossi domain (West African Craton) – regional and global context. Lund University – Lithosphere and Paleobiosphere Sciences. 2014;375(45 hskp/ECTS).
20. Jessell MW, Begg GC, Miller MS. The geophysical signatures of the West African Craton. Precambrian Res, Craton to Regional-scale analysis of the Birimian of West Africa. 2016;274 : 3–24. Available :https://doi.org/10.1016/j.precamres 2015; 08.010.
21. Milési JP, Feybesse JL, Pinna P. Geological map of Africa 1:10000000, SIGAfrique project. In: 20th Conference of African Geology, BRGM, Orléans. 2004; France, June 2–7.
22. Eglinger A, Thébaud N, Zeh A, Davis J, Miller J, Parra-Avila LA, Loucks R, McCuaig C. New insights into the crustal growth of the Paleoproterozoic margin of the Archean Kenema- Man domain, West African craton (Guinea): Implications for gold mineral system. Precambr. Res. https://doi.org/10.1016/j. precam.res. 2017;11.012.
23. Kitson AE. Provisional Geological Map of the Gold Coast and Western Togoland with Brief Descriptive Notes Thereon 19 Plates: By Sir Albert E. Kitson. Benham & Company ; 1928.
24. Junner NR. The geology of the gold coast and western togoland with revised geological map (1000000). Gold Coast geol. Surv. Bull. 1940;11(40).
25. Bessoles B. Geology of Africa, the West African craton Mém. B.R.G.M., Paris. 1977;88 :402.
26. Caby R, Delor C, Agoh O. Lithology, structure and metamorphism of Birimian formations in the Odienné region (Ivory Coast): Major role of pluton diapirism and strike-slip at the edge of the craton Man. J. Afr. Earth Sci. 2000;30 :351-374.
27. Camil J. An example of prograde metamorphism from the base of the amphibolite facies to the granulite facies in the Man region (Western Ivory Coast), reports Rendus l'Académie Sci. Paris 1981;293 :513-518.
28. Gouedji F, Picard C, Coulibaly Y, Audet MA, Auge T, Goncalves P, Paquette JL, Ouattara N. The samapleu maficeultramafic intrusion and its Ni-Cu-PGE mineralization: an Eburnean (2.09 Ga) feeder dike to the Yacouba layered complex (Man Archean craton, western Ivory Coast). Bull. Soc. Geol. 2014;185:393-411.
29. Pitra P, Kouamelan AN, Ballevre M, Peucat JJ. Paleoproterozoic high pressure granulite overprint of the Archean continental crust: evidence for homogeneous crustal thickening (Man Rise. Ivory Coast). Journal of metamorphic geology. 2010;28 :41-58.
30. Abouchami W, Boher M, Michard A, Albarède F, Major A. 2.1-Ga event of mafic magmatism in west Africa: An early stage of crustal accretion, J. Geophys. Res. 1990;95:7605–17629.
31. Baratoux L, Metelka V, Naba S, Jessel MW, Gregoire M, Ganne J. Juvenile Paleoproterozoic crust evolution during the

Eburnean orogeny (~2.2-2.0 Ga), western Burkina Faso. Prec. Res., 2011;191:18-45.
32. Feybesse JL, Billa M, Guerrot C, Duguey E, Lescuyer JL, Milesi JP, Bouchot V. The paleoproterozoic Ghanaian province: Geodynamic model and ore controls , including regional stress modeling. Precambrian Research, 2006;149(3):149–196.
33. Gasquet D, Barbey P, Adou M, Paquette JL. Structure Sr-Nd isotope geochemistry and zircon U–Pb geochronology of the granitoids of the Dabakala area (Côte d'Ivoire): evidence for a 2.3 Ga crustal growth event in the Palaeoproterozoic of West Africa? Precambrian Research. 2003; 127:329–354.
34. Alric G. Contribution to the petrographic study of Birrimian non-granitoid magmatic rocks of Haute-Comoé (NE of Ivory Coast). Ann. Univ. Abidjan, Series C, Sciences, volume XXI; 1985.
35. Arnould A. Geological study of Precambrian migmatites and granites of northern Ivory Coast and southern Upper Volta. Same. BRGM. 1961;174.
36. Alric G, Gibert P, Vidal M. The problem of the Birimian graywackes of Ivory Coast: A review and new data. The case of the Comoé unit. C.R. Acad. Sci. Paris, 1987;304:289-294.
37. Herron MM. Geochemical classification of terrigenous sands and shales from core, or log data. J.Sed. Petrol. 1988;58:820-829.
38. Larbi Y. Geochemical characterization (major elements and trace elements), isotopic tracing (Sm-Nd, Lu-Hf) and geochronology (Pb-Pb, U-Pb) of the wakeham group, n.e. Quebec: Proterozoic sedimentary basin in the Grenville province. Doctoral Thesis Res. minerals. Univ. Quebec. 2003;163.
39. Nesbitt H, Young G. Prediction of some weathering trends of plutonic and volcanic rocks based on thermodynamic and kinetic consideration. Geochimica Cosmochimica Acta 1984;48523-1534.
40. Fedo CM, Nesbitt HW, Young GM. Unraveling the effects of potassium metasomatism in the sedimentary rocks and paleosols with implications for paleoweathering conditions and provenance. Geology. 1995;23:921-924.
41. Aristizábal E, Roser B, Yokota S. Patterns and indices of chemical meteorization of vertical deposits and rock sources in the Valley of Aburrá. Boletín de Ciencias de la Tierra. 2009;(25): 27-42.
42. Doyon J. Comparison of the composition of Archean metasedimentary rocks in six basins of the Superior Province: A geochemical and statistical study. Same. Masters in Earth Sciences Univ. Quebec. 2004;271.
43. Deer WA, Howie RA, Zussman J. An introduction to the rock-forming minerals. Mineralogical Society of Great Britain and Ireland, 3rd edition. 2013;507.
44. Sun SS, McDonough WF. Chemical and isotopic systematics of oceanic basalts: Implication for mantle composition and processes. In: Saunders, A.D., Norry, M.J. (Eds.), Magmatism in Ocean Basins, vol. 42. Geological Society of London Special Publication. 1989;313–345.
45. McLennan SM, Taylor SR. Th and Uin sedimentary rocks: Crustal evolution and sedimentary recycling. Nature (London). 1980;285:621-624.
46. Bathia MR, Crook AW. Trace element characteristics of greywackes and tectonic setting discrimination of sedimentary basins. Contribution to Mineralogy and Petrology, 1986;92:181-193
47. Koffi YA, Kouamelan AN, Kouadio FJLH, Teha KR, Kouassi BR, Koffi GRS. Petrography and origin of metasediments from the SASCA domain (SW Ivory Coast). International Journal of Innovation and Applied Studies. 2018;23:451-464.
48. Asiadu DK, Dampare S, Asamoah-Sakyi P, Banoeng-Yakubo B, Osae S, Nyarko BJB, Manu J. Geochemistry of Paleoproterozoic metasedimentary rocks from the Birim diamondiferous field, southern Ghana: Implications for provenance and crustal evolution at the Archean-Proterozoic boundary. Geochem. J. 2004;38:215–2.
49. Duparc Q, Cousineau P, Bandyayera D. Correlation of the sedimentary basins of the northeast of the La Grande Subprovince (James Bay), using lithological and mineral geochemistry. Ministry of Natural Resources; GM 66440. 2012;37.
50. Fleet AJ. Aqueous and sedimentary geochemistry of the rare earth elements. Henderson P. (eds.), Rare earth element geochemistry. Elsevier. 1984 ;343-349.
51. Mclennan SM. Rare earth elements in sedimentary rocks: Influence of provenance and sedimentary processes. Lipin B.R. and McKay G.A. (eds),

Geochemistry and mineralogy of rare earth elements. Reviews in Mineralogy. 1984;21:169-200

52. Rollinson HR. Using Geochemical Data: Evaluation, Presentation, Interpretation. Longman Group UK Limited, London. 1993;252.
53. Asiadu DK, Asong S,Atta-Peters D, Sakyia P, Ben-Xun Suc,Dampared S, Chris Y, Anania C, Geochemical and Nd-isotopic compositions of juvenile-type Paleoproterozoic Birimian sedimentary rocks from southeastern West African Craton (Ghana): Constraints on provenance and tectonic setting. Precambrian Research. 2017;300:40-52.
54. Saxena A, Pandit MK, Zhao JH. Geochemistry of Hindoli Group Metasediments, SE Aravalli Craton, NW India: Implications on Provenance Characteristics and Tectonic Setting. Journal of the Geological Society of India. 2023 Aug;99(8):1071-82.
55. Houssou NN. Petrological, structural and metallogenic study of the Agbahou gold deposit, Divo, Ivory Coast. Doctoral thesis Univ. Félix Houphouët-Boigny. Abidjan, 2013;176.
56. Allou G. Study of the volcano-sedimentary series in the Dabakala region (Northeast Ivory Coast): genesis and magmatic evolution. Contribution to the knowledge of the gold mineralization of Bobosso in the Haute-Comoé series. Doctoral Thesis, Univ. Paris-Sud Orsay, France and Univ.Félix Houphouët-Boigny, 2014;303.
57. Kouadio FJLH, Cherubin DS, Nicaise KA, Ephrem AM, Koffi YA. Petrographical and geochemical signatures of paragneisses of Tabou and Grand-Bereby sectors (south-west of Ivory Coast). International Journal of Innovation and Applied Studies. 2016;18(3):646.
58. Hifzurrahman, Nasipuri P, Joshi KB. Geochemistry of Jutogh Metasediments, Lesser Himachal Himalaya, India, and their Implications in Source Area Weathering, Provenance, and Tectonic Setting during Paleoproterozoic Nuna Assembly. Journal of the Geological Society of India. 2023 Jul; 99(7):897-905.
59. Kovach VP, Adamskaya EV, Kotov AB, Berezkin BI, Timofeev VF, Popov NV, Plotkina YV, Skovitina TM, Fedoseenko AM, Zagornaya NY, Gorokhovsky BM. Sources of the Paleoproterozoic Terrigenous Rocks of the Nizhnekhani Graben-Syncline, Western Part of the Aldan Shield, According to the U–Th–Pb (LA-ICP-MS) Geochronological and Nd Isotopic Studies: To the Question of Correlation of the Udokan Complex Deposits. Stratigraphy and Geological Correlation. 2023 Oct;31(5):376-89.

Peer-review history:
The peer review history for this paper can be accessed here:
https://www.sdiarticle5.com/review-history/107166